

## SO(2N) and SU(N) gauge theories in 2+1 dimensions

Francis Bursa,<sup>a</sup> Richard Lau<sup>b</sup> and Michael Teper<sup>b</sup>

<sup>a</sup>*Physics Department, Swansea University,  
Swansea SA2 8PP, U.K.*

<sup>b</sup>*Rudolf Peierls Centre for Theoretical Physics, University of Oxford,  
1 Keble Road, Oxford OX1 3NP, U.K.*

*E-mail:* [f.bursa@swansea.ac.uk](mailto:f.bursa@swansea.ac.uk), [r.lau1@physics.ox.ac.uk](mailto:r.lau1@physics.ox.ac.uk),  
[m.teper1@physics.ox.ac.uk](mailto:m.teper1@physics.ox.ac.uk)

ABSTRACT: We perform an exploratory investigation of how rapidly the physics of SO(2N) gauge theories approaches its  $N = \infty$  limit. This question has recently become topical because SO(2N) gauge theories are orbifold equivalent to SU(N) gauge theories, but do not have a finite chemical potential sign problem. It is therefore interesting to know how close is the physics of SO(N) to that of SU(3) for the modest values of  $N$  where one might be able to perform chemical potential calculations. We consider only the pure gauge theory and, because of the inconvenient location of the lattice strong-to-weak coupling 'bulk' transition in 3+1 dimensions, we largely confine our numerical calculations to 2+1 dimensions in this paper. We provide some analytic estimates of the SO(2N) spectrum in both  $D = 2 + 1$  and  $D = 3 + 1$ , and show, numerically, that the  $D = 2 + 1$  SO(6) and SU(4) low-lying spectra do indeed appear to be the same. Our numerical calculations of a number of mass ratios show that the leading  $O(1/N)$  correction already dominates for  $N \geq 6$ , and in some cases down to  $N = 4$ , and that, as expected, these ratios become consistent with those of SU(N) as  $N \rightarrow \infty$ . In particular we see that SO(6) and SU(3) gauge theories are quite similar except for the values of the string tension and coupling, both of which differences can be readily understood.

KEYWORDS: Lattice Gauge Field Theories, 1/N Expansion

ARXIV EPRINT: [1208.4547](https://arxiv.org/abs/1208.4547)

---

**Contents**

<b>1</b>	<b>Introduction</b>	<b>1</b>
<b>2</b>	<b>Expectations</b>	<b>3</b>
2.1	General remarks	3
2.2	SO(6), SU(4) and SO(2N)	4
2.3	SO(3) and SU(2)	7
<b>3</b>	<b>Calculations in D=2+1</b>	<b>7</b>
3.1	Calculating on the lattice	7
3.2	Bulk transition	8
3.3	SO(6) and SU(4)	10
3.4	The deconfining transition	14
3.5	Continuum mass ratios	15
<b>4</b>	<b>D=3+1</b>	<b>19</b>
<b>5</b>	<b>Conclusions</b>	<b>21</b>

---

**1 Introduction**

SO( $2N$ ) gauge theories are of topical interest because they do not suffer a finite chemical potential sign problem [1], are orbifold equivalent [2–4] to SU( $N$ ) gauge theories [1, 5] and share with the latter a common large  $N$  limit in their common sector of states (see [6] for an early derivation and [7] for a recent pedagogical one). Thus if SU(3) and, say, SO(6) are both close to  $N = \infty$ , then the finite baryon density phase diagram in QCD might be illuminated by lattice Monte Carlo calculations of, say, SO(6) [1].

This has motivated us to study the pure gauge theories, as a first step. In this case much is known about SU( $N$ ) both in D=3+1 [8–10] and in D=2+1 [11, 12], and our calculations have therefore focused upon SO( $N$ ). As shown below, if one uses the standard plaquette action then the strong-to-weak coupling ‘bulk’ phase transition in D=3+1 SO( $N$ ) gauge theories occurs at such a small value of the lattice spacing  $a$ , when  $N$  is not large, that it becomes prohibitively expensive to perform weak coupling calculations in volumes that are large enough to be in the confining phase. (This has long been known in the extreme case of SO(3). For a recent study see [13].) To deal with this problem, we are currently exploring improved actions in the hope that the bulk transition may be shifted to stronger coupling. In D=2+1 on the other hand, the strong-to-weak coupling transition provides much less of an obstacle and so most of the lattice calculations in the present paper will deal with SO( $N$ ) gauge theories in 2+1 dimensions.

There are of course additional reasons for being interested in  $SO(N)$  gauge theories. For example, an  $SO(N)$  gauge theory can have exactly the same Lie algebra as some  $SU(N')$  theory. This is the case for  $SO(3)$  and  $SU(2)$  and also for  $SO(6)$  and  $SU(4)$ . One would expect the two theories in each pair to have the same spectrum in the continuum limit, assuming the global properties of the group do not play a role in the dynamics. It would be nice to check this expectation, and we shall provide evidence later on in this paper that this is indeed the case for  $SU(4)$  and  $SO(6)$ . This will enable us to make an approximate prediction for the  $N$ -dependence of  $SO(N)$  gauge theories for  $N \geq 6$  in both 2+1 and 3+1 dimensions, using the known properties of the  $SU(4)$  gauge theory.

Although our calculations are still at an early stage, the results we have obtained provide useful information on the above questions and we will present these below. We will also discuss in detail how to compare physical quantities in  $SU(N)$  and  $SO(2N)$  gauge theories. We will present results for the string tension,  $\sigma$ , the lightest two  $J^P = 0^+$  scalar states, the lightest  $J^P = 2^+$  tensor, the deconfining temperature  $T_c$ , and the coupling  $g^2$ , which in  $D=2+1$  has dimensions of mass. We do so for  $SO(4)$ ,  $SO(6)$ ,  $SO(8)$  and  $SO(12)$  gauge theories, and use these results to test the large- $N$  equivalence with  $SU(N)$  and to determine the rate of approach to that limit.

Since our primary focus here is on the  $SO(2N)$  and  $SU(N)$  equivalence, we do not discuss  $SO(2N+1)$  gauge theories, which differ from  $SO(2N)$  in that they lack the (useful)  $Z_2$  center symmetry of the latter. We will leave our detailed comparison of  $SO(3)$  and  $SU(2)$  to a separate paper and will include our ongoing detailed study of odd  $N$  to a future publication. We merely note here that our first glance at the physics of  $SO(2N+1)$  gauge theories suggests that it is entirely continuous with that of neighbouring  $SO(2N)$  gauge theories.

In the next section we review some expectations about the large- $N$  limit. We also discuss how precisely the calculated physics of  $SO(6)$  and  $SU(4)$  gauge theories is to be identified. (And separately the case of  $SU(2)$  and  $SO(3)$ .) We note that this equality provides approximate predictions for the  $N$ -dependence of  $SO(N)$  gauge theories in both  $D=2+1$  and  $D=3+1$ . The following section contains our calculations. We outline the lattice calculation and then locate the strong-to-weak coupling transition in both  $D=3+1$  and  $D=2+1$ . We show that in the former case it is only for  $N \geq 16$  that one can obtain useful weak-coupling physics on reasonably sized lattices. Focusing on  $D=2+1$  we provide a detailed calculation for  $SO(6)$  and compare the continuum extrapolation to  $SU(4)$ . We then extrapolate to the continuum our calculations for other values of  $N$ . Here our calculations are currently much more limited and we need to justify the reliability of these extrapolations using what we find in  $SO(6)$ .

It is worth listing some of the ways in which our work in progress [14] will improve upon the  $D=2+1$  results presented here. First, we will perform calculations at smaller  $a$  so as to reduce the systematic error on our continuum extrapolations. We will also include  $P = -$  states. (Recall that in  $D=2+1$   $J^\pm$  states are degenerate except possibly for  $J = 0$ .) We will include  $J = 1$  states as well as  $J = 0, 2$ . All this will provide a larger spectrum of states, calculated with greater precision. We also intend to perform the calculations of  $T_c$  much more accurately using standard reweighting methods that have been used in the case

of  $SU(N)$  (see e.g. [15–19]). We will include  $SO(2N + 1)$  gauge theories in all these studies. Finally, for a useful comparison it may also prove necessary to repeat the corresponding  $SU(N)$  calculations with greater accuracy than that currently available.

More speculatively we hope that our lattice action improvement will enable us to obtain  $SO(N)$  continuum physics in  $D=3+1$  for the modest values of  $N$  where finite chemical potential calculations might conceivably be performed. In addition it would be of interest to study the spinorial representations particularly in the context of the corresponding flux tubes and string tensions.

## 2 Expectations

### 2.1 General remarks

As is well known, the analysis of diagrams to all orders tells us [20] that the large  $N$  limit of  $SU(N)$  gauge theories is achieved by keeping  $g^2 N$  fixed and that the leading correction in the pure gauge theory is  $O(1/N^2)$ . A parallel analysis for  $SO(N)$  gauge theories tells us [7] that  $g^2 N$  should be kept fixed but that the leading correction is  $O(1/N)$ . Moreover the  $N = \infty$  limit of the two theories is the same if we choose the  $SO(N)$  value of  $g^2$  to be twice the  $SU(N)$  value,

$$g^2|_{SO(N)} \stackrel{N \rightarrow \infty}{\equiv} 2 \times g^2|_{SU(N)} \tag{2.1}$$

or equivalently if we match  $SO(2N)$  and  $SU(N)$  theories at the same coupling. There exists a corresponding orbifold equivalence [1, 5].

Of course  $SO(N)$  gauge theories have trivial charge conjugation properties and therefore the comparison with  $SU(N)$  is only in the  $C = +$  sector. The two groups also differ qualitatively in their symmetry properties: even where  $SU(N')$  and  $SO(N)$  gauge theories are equivalent at the level of the Lie algebra, their global properties differ. For example,  $SU(4)$  has a  $Z_4$  center while  $SO(6)$  has only  $Z_2$  while in the pair  $SU(2)$  and  $SO(3)$  the former has a  $Z_2$  center while the latter has a trivial center. Large fields may be sensitive to the global properties and it is therefore interesting to test the expectations of the diagrammatic equivalences at the non-perturbative level using lattice Monte Carlo techniques.

Matching physical quantities in  $SO(N)$  and  $SU(N')$  gauge theories is straightforward for colour singlet quantities, such as ‘glueball’ masses. For flux tubes and string tensions, however, one needs to be more careful. Suppose one considers a flux tube that wraps around a spatial torus of length  $l$ . For  $l$  large the calculated energy gives the string tension via  $E \simeq \sigma l$ . In  $SU(N)$  there are a variety of stable flux tubes labelled by the value  $k = 1, 2, \dots, N/2$  of their  $\mathcal{N}$ -ality, and other unstable flux tubes, such as the adjoint flux tube, carrying flux in various representations. In the case of  $SU(2)$  and  $SO(3)$ , it is well known that the latter is equivalent to the former in the adjoint representation. Thus  $SO(3)$  flux tubes correspond to  $SU(2)$  flux tubes that carry adjoint flux, which indeed have  $C = +$ . The latter are of course unstable, and can decay into glueballs, but this is consistent with the fact that  $SO(3)$  does not possess a non-trivial center which would prevent the mixing of a winding flux tube operator with contractible operators that project onto glueball states. Thus the  $\sigma$  extracted in  $SO(3)$  corresponds to the adjoint string tension in  $SU(2)$ . Since

we are interested in  $SO(2N)$ , we will not pursue the  $SO(3) \sim SU(2)$  correspondence any further here, but will leave it to a future publication. The  $SU(4) \sim SO(6)$  correspondence is however relevant and that will be discussed below. More generally we note that the  $Z_2$  center of  $SO(2N)$  ensures that these theories have stable flux tubes just like  $SU(N)$ . Of course for  $2N + 1 \geq 5$  we may expect, by continuity, that  $SO(2N + 1)$  theories also have stable flux tubes, but if so (and our preliminary calculations indicate that this is indeed the case) then it will be enforced by dynamics rather than an explicit non-trivial center symmetry. Indeed it is known that as  $N \rightarrow \infty$  an emergent  $Z_N$  center symmetry does get dynamically restored [21] in a class of field theories that includes  $SO(N)$ .

## 2.2 $SO(6)$ , $SU(4)$ and $SO(2N)$

As is well known,  $SU(4)$  and  $SO(6)$  have the same Lie algebra, so one expects that the  $C = +$  glueball spectra will be identical. Now we recall that in  $SU(4)$

$$\underline{4} \otimes \underline{4} = \underline{6} \oplus \underline{10} \tag{2.2}$$

(see e.g. [22]) where the  $\underline{6}$  corresponds to the  $k = 2$  antisymmetric representation (which indeed is  $C = +$  for  $SU(4)$ ) and maps to the fundamental  $\underline{6}$  of  $SO(6)$ . Thus in the equivalence with  $SO(6)$  we are to think of  $k = 2A$  operators in  $SU(4)$  and the  $SO(6)$  string tension should be compared to the  $k = 2A$  string tension in  $SU(4)$ . In terms of the fundamental  $SU(4)$  string tension this has values

$$\frac{\sigma_{2A}}{\sigma_f} = \begin{cases} 1.355 \pm 0.009 & D = 2 + 1 \\ 1.370 \pm 0.020 & D = 3 + 1 \end{cases} \tag{2.3}$$

in  $D = 2 + 1$  [23, 24] and  $D = 3 + 1$  [10]. This implies that we should compare mass ratios as:

$$\left. \frac{M_G}{\sqrt{\sigma}} \right|_{so6} = \left. \frac{M_G}{\sqrt{\sigma_{2A}}} \right|_{su4} \tag{2.4}$$

For example, consider the lightest scalar glueball in  $D=2+1$   $SU(4)$ . Using the known value of the ratio in  $SU(4)$  [11, 12] we obtain the corresponding ratio in  $SO(6)$ :

$$\left. \frac{M_G}{\sqrt{\sigma}} \right|_{so6} = \left. \frac{M_G}{\sqrt{\sigma_f}} \right|_{su4} \times \sqrt{\left. \left\{ \frac{\sigma_f}{\sigma_{2A}} \right\} \right|_{su4}} = \frac{4.235(25)}{1.164(4)} = 3.638(25) \tag{2.5}$$

We also expect that at  $N = \infty$ ,

$$\left. \frac{M_G}{\sqrt{\sigma}} \right|_{so(\infty)} = \left. \frac{M_G}{\sqrt{\sigma_f}} \right|_{su(\infty)} = 4.108(20) \tag{2.6}$$

If we now assume that the leading  $O(1/N)$  correction dominates for  $N \geq 6$ , i.e.

$$\left. \frac{M_G}{\sqrt{\sigma}} \right|_{so(N)} \simeq \left. \frac{M_G}{\sqrt{\sigma}} \right|_{so(\infty)} + \frac{c}{N} \quad ; \quad N \geq 6 \tag{2.7}$$

we can use eqs. (2.6), (2.5) to determine the coefficient  $c$  in eq. (2.7) and hence the ratio for all values of  $N \geq 6$ . We display this prediction in figure 1, with  $c \simeq 2.8$ , where we

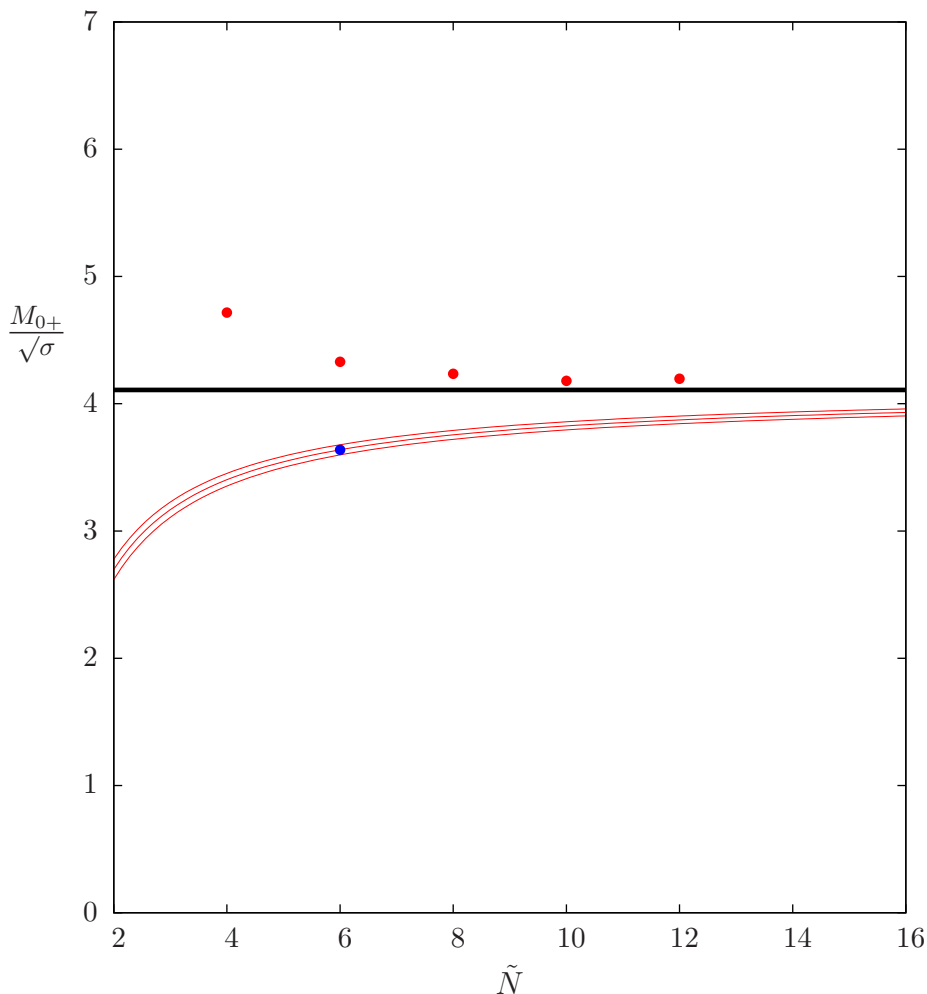


**Figure 1.** Mass of lightest glueball in units of the string tension  $\sigma$ . Curves are predictions (with error band) for  $\text{SO}(\tilde{N})$  assuming just the leading  $O(1/\tilde{N})$  correction and equality of spectra for  $\text{SO}(6)$  and  $\text{SU}(4)$  and  $\text{SO}(\infty)$  and  $\text{SU}(\infty)$  as described in the text. Red points are  $\text{SU}(N)$  values at  $N = \tilde{N}/2$ .

also display the  $\text{SU}(N)$  values of the ratio [11, 12], and the value predicted for  $\text{SO}(6)$  in eq. (2.5). We see that this ratio approaches the  $N = \infty$  limit from opposite sides for  $\text{SO}(N)$  and  $\text{SU}(N)$ . This is driven by the fact that in the denominator of this ratio we have  $\sqrt{\sigma}|_{so6} = \sqrt{\sigma}_{2A}|_{su4} \simeq 1.164\sqrt{\sigma}|_{su4}$ . The important corollary is that even if our assumption of the dominance of the  $O(1/N)$  correction is inaccurate, the qualitative behaviour shown in figure 1 is almost certain to survive.

We can obviously extend the above argument to any glueball mass ratio: assume the dominance of the leading  $O(1/N)$  correction for  $N \geq 6$ , then use existing  $\text{SU}(4)$  and  $\text{SU}(\infty)$  results [8–12, 23, 24] to fix the mass ratio for  $\text{SO}(6)$  and  $\text{SO}(\infty)$ , and hence predict the ratio for all  $\text{SO}(N \geq 6)$ . It is clear that the difference between  $\text{SU}(N)$  and  $\text{SO}(N)$  for such glueball mass ratios is certain to be far more modest than for  $M_G/\sqrt{\sigma}$ . For example,

$m_{2+}/m_{0+}$  and  $m_{0+*}/m_{0+}$  change by less than 1% when we go from SU(4) to SU( $\infty$ ) [10–12] and hence also when we go from SO(6) to SO( $\infty$ ). Short of some fine-tuned cancellation between the  $O(1/N)$  and  $O(1/N^2)$  corrections for SO(6), the near constancy of these mass ratios for SO( $N \geq 6$ ) is thus more-or-less guaranteed. The same comment applies to the location of the deconfining temperature  $T_c$  if expressed in units of the mass gap.

Irrespective of these arguments for larger  $N$ , the fact that such energy ratios are known to be very similar for SU(3) and SU(4) immediately implies the same for SU(3) and SO(6), i.e. in the case of particular interest to the finite chemical potential problem [1, 7]. (We focus here on the pairing of SU(3) and SO(6) because of the large- $N$  orbifold equivalence of SU( $N$ ) and SO( $2N$ ) gauge theories. However we should bear in mind that other SO( $N$ ) theories that are sufficiently ‘close’ to SU(3) may be useful — either because they are less expensive, e.g. SO(4), or because they have a less severe bulk transition problem, e.g. SO(12) in D=3+1.)

In D=2+1 the coupling  $g^2$  has dimensions of mass, and so we can consider ratios of  $\mu/g^2N$  for some physical mass  $\mu$ , and ask how this ratio approaches the  $N = \infty$  limit where, from eq. (2.1), one expects that  $g^2|_{soN} = 2g^2|_{suN}$ . Consider SO(6). The large  $N$  expectation [7, 20] would be that

$$g^2|_{so6} = 2g^2|_{su6} = 2 \times \frac{2}{3}g^2|_{su4} = \frac{4}{3}g^2|_{su4} \tag{2.8}$$

up to  $O(1/N)$  corrections. On the other hand, we know that the SO(6) action is equivalent to working in SU(4) with the fields in the  $k = 2A$  representation, and this should predict the precise relation between the SU(4) and SO(6) couplings. To proceed let us can think of a mixed SU(4) lattice plaquette action

$$S = \beta_f \sum_p \left\{ 1 - \frac{1}{N_f} \text{ReTr}_f u_p \right\} + \beta_{2A} \sum_p \left\{ 1 - \frac{1}{N_{2A}} \text{Tr}_{2A} u_p \right\} \tag{2.9}$$

where

$$\beta_f = 2N_f/g_f^2 \quad ; \quad \beta_{2A} = 2N_{2A}/g_{2A}^2 \tag{2.10}$$

just like a more conventional mixed fundamental-adjoint action. We have added here a subscript  $f$  to the usual (fundamental)  $g^2$  for clarity. For SU(4), the sizes of the representations are  $N_f = 4$ ,  $N_{2A} = 6$ . Using

$$\text{Tr}_{2A} u_p = \frac{1}{2} \{ (\text{Tr}_f u_p)^2 - \text{Tr}_f u_p^2 \} \tag{2.11}$$

and performing a weak coupling expansion one readily sees that the correct relation between the SO(6) and SU(4) couplings is

$$g^2|_{so6} = g_{2A}^2|_{su4} = 2g_f^2|_{su4}. \tag{2.12}$$

This differs from the large- $N$  expectation in eq. (2.8) by a factor of 1.5, implying that here, just as with the string tension, there are quite substantial finite  $N$  corrections.

We can conclude from the above general arguments that the comparison between SU(3) and SO(6) is as follows: ratios of glueball masses and  $T_c$  are very similar, while ratios involving the string tension and the coupling will typically differ at the 15 – 20% level.

Of course, all the above assumes that the different global properties of the SU(4) and SO(6) groups plays no important role in the details of the spectrum. This is something that we shall explicitly check for the lightest masses below.

### 2.3 SO(3) and SU(2)

Although we do not study SO(2N+1) theories in this paper, it is relevant to note that, using the fact that SO(3) is the adjoint of SU(2), one can further constrain the  $N$ -dependence of SO( $N$ ) gauge theories, using the known properties of SU(2) gauge theories. Together with the constraint from SO(6) and SU(4) this allows us to fix both the  $O(1/N)$  and  $O(1/N^2)$  corrections if we assume that these dominate down to SO(3). Care is needed with the string tension, since the SU(2) adjoint string is unstable, but ratios involving glueball masses,  $T_c$ , and  $g^2$  can be treated straightforwardly by an obvious extension of the analysis in section 2.2.

## 3 Calculations in D=2+1

### 3.1 Calculating on the lattice

Our lattice field variables are SO( $N$ ) matrices,  $U_l$ , residing on the links  $l$  of the  $L_s^2 L_t$  lattice, whose spacing is  $a$ . (We will employ the same notation as used for unitary matrices although here the matrices are of course real.) The Euclidean path integral is  $Z = \int \mathcal{D}U \exp\{-S[U]\}$  and we use the standard plaquette action,

$$S = \beta \sum_p \left\{ 1 - \frac{1}{N} \text{Tr} U_p \right\} \quad ; \quad \beta = \frac{2N}{ag^2} \tag{3.1}$$

where  $U_p$  is the ordered product of link matrices around the plaquette  $p$ . We update the fields using a natural extension to SO( $N$ ) of the SU( $N$ ) Cabibbo-Marinari algorithm. (The details of this algorithm will be described elsewhere [14].)

Our SO( $N$ ) calculations closely parallel those in SU( $N$ ), so we will be very brief here and will refer the reader to other papers for details.

The particle ('glueball') states can be labelled by parity  $P = \pm$  and spin  $J$ . (Charge conjugation is necessarily positive.) For  $J \neq 0$  the  $P = \pm$  states are necessarily degenerate in  $D = 2 + 1$  [11, 12] and in this exploratory study we shall only calculate the masses of  $P = +$  and  $J = 0, 2$  states. Here we will make the usual simplifying assumption that the states we see have the lowest  $J$  that contributes to the relevant square lattice representation. (This is usually but not always the case [25].)

Ground state masses  $M$  are calculated from the asymptotic time dependence of correlators, i.e.

$$\langle \phi(t)\phi(0) \rangle \underset{t \rightarrow \infty}{\sim} e^{-Mt} \tag{3.2}$$



where  $M$  is the mass of the lightest state with the quantum numbers of the operator  $\phi$ . To calculate excited states as well one calculates (cross)correlators of several operators and uses these as a basis for a systematic variational calculation in  $e^{-Ht_0}$  where  $H$  is the Hamiltonian (corresponding to our lattice transfer matrix) and  $t_0$  is some convenient distance. To have good overlaps onto the desired states, so that one can evaluate masses at values of  $t$  where the signal has not yet disappeared into the statistical noise, one uses blocked and smeared operators. (For details see e.g. [10–12].)

To calculate the string tension  $\sigma$  we use the above technique to calculate the energy  $E$  of the lightest flux tube that winds around one of the periodic spatial tori. If the length  $l = aL_s$  of the torus is large then  $E(l) \simeq \sigma l$  where  $\sigma$  is the string tension. There are of course corrections and we assume that for our range of  $l$  these are accurately incorporated in the simple Nambu-Goto expression

$$E(l) = \sigma l \left\{ 1 - \frac{\pi}{3\sigma l^2} \right\}^{1/2} \tag{3.3}$$

which is what we shall use to extract  $\sigma$  from  $E(l)$ . (See e.g. [26–28] and references therein.) The operator we use is the Polyakov loop  $l_p$ , i.e. the product of link matrices along a minimal length curve that closes around the spatial torus. (And blocked versions of this.) For even  $N$ , which is the case of interest in this paper, the theory has a  $Z_2$  symmetry that ensures that  $\langle l_p \rangle = 0$  as long as the symmetry is not spontaneously broken, and indeed that  $\langle l_p \phi_G \rangle = 0$  where  $\phi_G$  is any contractible loop (which is what one uses for glueball operators). That is to say we have a stable flux tube state that winds around the torus.

We can similarly consider Polyakov loop operators that wind around the temporal torus on our  $L_s^2 L_t$  lattice. Such a finite torus corresponds to a finite temperature  $T = 1/aL_t$  if we are in the thermodynamic limit  $L_s \gg L_t$ . The Polyakov loop is the contribution to the action of a single charged static source. Just as above, the  $Z_2$  symmetry ensures that  $\langle l_p \rangle = 0$ , i.e. that the free energy of the static source is infinite, if we are in the low temperature confining phase. As we decrease  $L_t$  at some temperature  $T = T_c$  the  $Z_2$  symmetry spontaneously breaks, we have  $\langle l_p \rangle \neq 0$  and we enter the deconfined phase where we have Debye screening and the source has a finite free energy.

### 3.2 Bulk transition

Lattice gauge theories generally show a (‘bulk’) transition between the strong and weak coupling regions where the natural expansion parameters are  $\beta \propto 1/g^2$  and  $1/\beta \propto g^2$  respectively. Since the extrapolation to the continuum limit should be made within the weak coupling region, it is important that the bulk transition should occur at a value of  $\beta$  where  $a$  on the weak coupling side is not very small. Otherwise prohibitively large lattices may be needed to ensure that one is in the weak coupling confining phase.

For D=3+1 SU( $N$ ) gauge theories it is known that the transition is first order for  $N \geq 5$  and is a cross-over for smaller  $N$  [8, 9]. In D=2+1 it appears to [29] be quite similar to the Gross-Witten transition in D=1+1 [30], i.e. a cross-over for all  $N < \infty$  developing into a third-order transition at  $N = \infty$ . The location in  $D = 3 + 1$  is such that on the weak coupling side we can readily go down to  $a \sim 1/5T_c$  (taking advantage

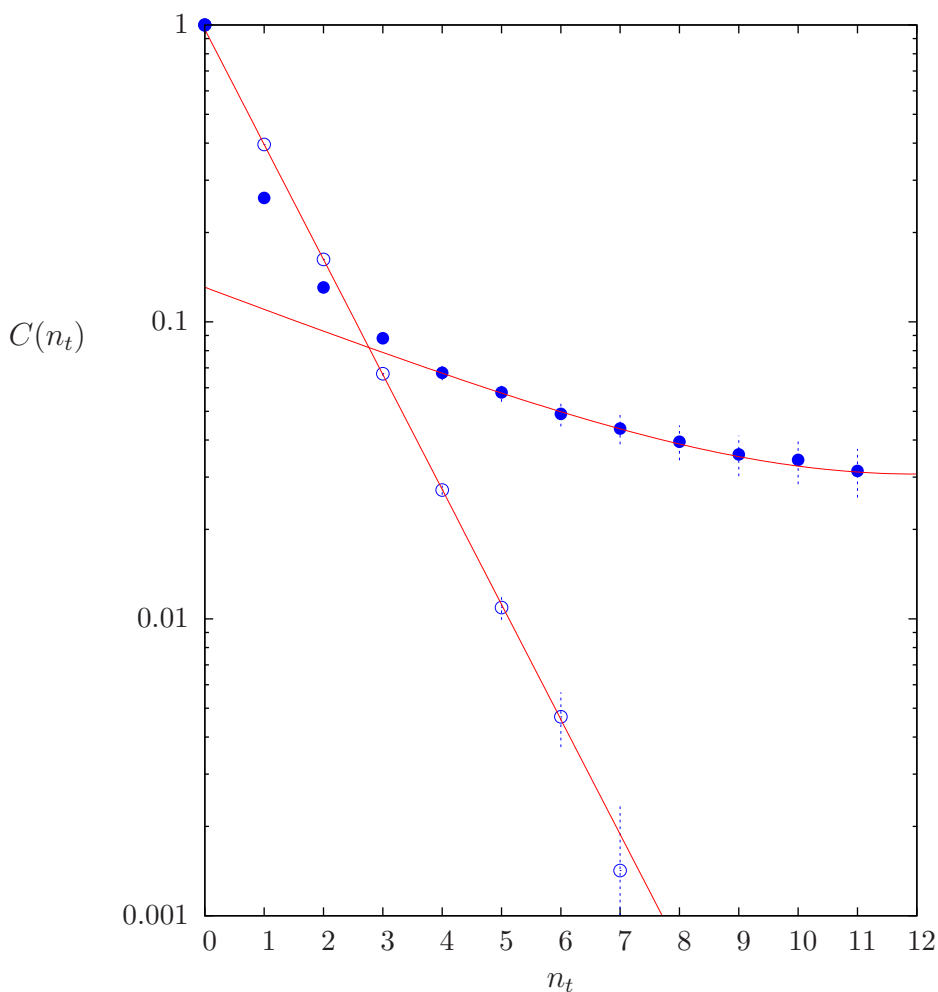


**Figure 2.** Correlation functions of the ‘lightest’,  $\circ$ , and ‘first excited’,  $\bullet$ ,  $0^+$  glueball states in  $SO(4)$  on a  $16^2 24$  lattice at  $\beta = 9.3$ . Single mass cosh fits are shown.

of the metastable region when the transition is first order). In  $D = 2 + 1$ , we can go to much larger  $a$ ,  $a \sim 1/1.6T_c$ . So in these cases the bulk transition presents no significant obstacle to continuum extrapolations. On the other hand it has long been known that for the  $D = 3 + 1$   $SU(2)$  theory in the adjoint representation, there is a bulk phase transition with a very small (and not precisely known) value of  $a$  on the weak coupling side. (For a recent discussion see [13].)

Since adjoint  $SU(2)$  is the same as  $SO(3)$ , this suggests that in  $D = 3 + 1$  the location of the bulk transition may be an obstacle to accessing the continuum limit of  $SO(N)$  gauge theories. We will address this in more detail later on in the paper. Here we turn to  $SO(N)$  gauge theories in  $D=2+1$ . We have performed scans in  $\beta$  for various  $N$  which show no sign of any first order transition. However we do find a transition which is characterised by a near-vanishing of a scalar glueball mass. The transition is in a narrow range of  $\beta$

SO(N) , D=2+1		
G	$(ag^2N)_b \sim$	$a\sqrt{\sigma} \sim$
SO(3)	3.0	0.164
SO(4)	3.44 - 3.76	0.265 - 0.308
SO(6)	3.74 - 4.06	0.364 - 0.428
SO(8)	3.85	0.423
SU( $\infty$ )	$\sim 2.2$	$\sim 0.7$

**Table 1.** Critical 't Hooft coupling for the D=2+1 bulk transition.

and its location depends slightly on the volume of the lattice. An example is shown in figure 2. Here we show the correlation functions of the two lightest glueballs as obtained from our variational procedure that maximises  $e^{-aH}$  over the basis of operators. The ‘lightest’ glueball is well fitted by a single cosh, showing that it has a very good overlap onto our basis. It is the state that is continuous with the lightest glueball masses away from the phase transition/cross-over. The ‘first excited state’, on the other hand, shows the presence of a very light particle that only shows up at larger  $n_t$  because it has a small overlap onto our basis. The presence of this light particle is the signal for the bulk transition. It is possible that we are seeing a nearby critical point, which might indeed be a second order phase transition at a nearby value of  $\beta$ . We have not investigated the nature of this transition or cross-over any further except to list in table 1 the values of the 't Hooft coupling,  $ag^2N = 2N^2/\beta$  at which we have observed it to occur. For comparison we show an estimate of the location for SU( $\infty$ ) theories [29]. We note that our results are roughly consistent with the naive orbifold expectation that  $g_b^2$  for SO( $2N$ ) and SU( $N$ ) lattice gauge theories should become the same as  $N \rightarrow \infty$  i.e. that the 't Hooft couplings should differ by a factor of 2. We also show the corresponding values of the string tension. We see that the transition occurs at a modest value of  $a$  in units of the string tension and so should present no significant obstacle to a continuum extrapolation.

### 3.3 SO(6) and SU(4)

In the case of SO(6) we have performed calculations over an extended range of  $a$ , designed to minimise any systematic error in performing the continuum extrapolation, so as to make our comparison with existing results for SU(4) reasonably reliable. The parameters of these calculations and some of the physical quantities calculated are shown in table 2.

As shown in table 2, we have performed calculations with various spatial volumes at  $\beta = 29$ , in order to determine how large a volume we need in order to avoid finite volume corrections (within the statistical errors characteristic of all our calculations). We observe no significant volume dependence for  $L_s \geq 16$  (at the level of 2 standard deviations). In physical units this lattice size corresponds to  $L_s a\sqrt{\sigma} \sim 3.4$ . We note that all the other calculations in table 2 which are beyond the bulk transition ( $\beta_b \sim 19$ ) have been chosen to satisfy this bound, and that the ones at the smallest values of  $a$  are considerably larger. So we expect finite volume corrections to be small in our continuum extrapolations.

SO(6) , D=2+1						
$\beta$	lattice	plaq	$a\sqrt{\sigma}$	$aM_{0+}$	$aM_{0+*}$	$aM_{2+}$
15.0	4 <sup>2</sup> 12	0.54264	0.678(3)	1.92(4)	—	—
15.15	6 <sup>2</sup> 12	0.55271	0.667(12)	1.872(28)	—	—
17.75	8 <sup>2</sup> 16	0.66735	0.4279(9)	1.521(11)	—	2.65(13)
18.0	8 <sup>2</sup> 16	0.67383	0.4161(14)	1.482(19)	—	2.72(19)
21.75	12 <sup>2</sup> 24	0.74255	0.3100(7)	1,1277(70)	1.696(23)	1.89(4)
22.0	12 <sup>2</sup> 16	0.74599	0.3053(8)	1.1122(52)	1.643(16)	1.940(28)
25.5	16 <sup>2</sup> 40	0.78553	0.2512(7)	0.9206(46)	1.391(10)	1.597(13)
29.0	12 <sup>2</sup> 48	0.81410	0.2108(5)	0.7517(42)	1.087(26)	1.299 (47)
29.0	16 <sup>2</sup> 48	0.81410	0.2150(4)	0.7872(42)	1.152(32)	1.394(18)
29.0	20 <sup>2</sup> 48	0.81410	0.2153(4)	0.7852(45)	1.183(27)	1.386(12)
29.0	24 <sup>2</sup> 32	0.81410	0.2155(6)	0.7770(51)	1.212(13)	1.405(14)
36.0	24 <sup>2</sup> 32	0.85294	0.1661(7)	0.6011(67)	0.947(7)	1.065(25)
48.0	32 <sup>2</sup> 40	0.89152	0.1205(4)	0.4489(36)	0.6667(72)	0.7709(93)

**Table 2.** Our D=2+1 SO(6) calculations with parameters and some calculated quantities.

Taking ratios of glueball masses to the string tension, we can attempt to extrapolate to the continuum limit using just a leading  $O(a^2)$  lattice correction

$$\frac{aM_G}{a\sqrt{\sigma}} \Big|_a = \frac{M_G}{\sqrt{\sigma}} \Big|_a \simeq \frac{M_G}{\sqrt{\sigma}} \Big|_{a=0} + ca^2\sigma. \tag{3.4}$$

In figure 3 we plot this ratio for the lightest two scalar glueballs and the lightest tensor glueball. (Note that the light scalar associated with the bulk transition at  $\beta \sim 18$  is deliberately excluded.) We show linear continuum extrapolations of the form in eq. (3.4) and these seem reasonably well determined. The resulting continuum mass ratios, obtained using values of  $\beta$  beyond the bulk transition, are listed in table 3. We have also shown there the values obtained from fits in which eq. (3.4) is supplemented by an additional  $O(a^4)$  correction. The difference between the pair of fits provides an estimate of one of the systematic errors in our continuum extrapolations. We also show the deconfining temperature whose calculation we leave to a later section. Finally, for comparison, we show the corresponding results for the SU(4) gauge theory [11, 12]. The agreement between SO(6) and SU(4) is very good at the 2 standard deviation level. This provides direct confirmation of the expected equivalence of the SU(4) and SO(6) spectra, and of our identification of the SO(6) string tension with the  $k = 2A$  string tension of SU(4).

There remains one major prediction to test: the relationship between the SO(6) and SU(4) couplings given in eq. (2.12). This can be done, for example, by calculating  $\sqrt{\sigma}/g^2$  in SO(6) and comparing it to the SU(4) value of  $\sqrt{\sigma_{2A}}/g^2$ . The former is then predicted by eq. (2.12) to be one-half of the latter. To obtain the SO(6) value of this ratio we perform the continuum extrapolation

$$\frac{\beta_I}{2N^2} a\sqrt{\sigma} \Big|_a \simeq \frac{\sqrt{\sigma}}{g^2 N} \Big|_{a=0} + \frac{c}{\beta_I} \tag{3.5}$$

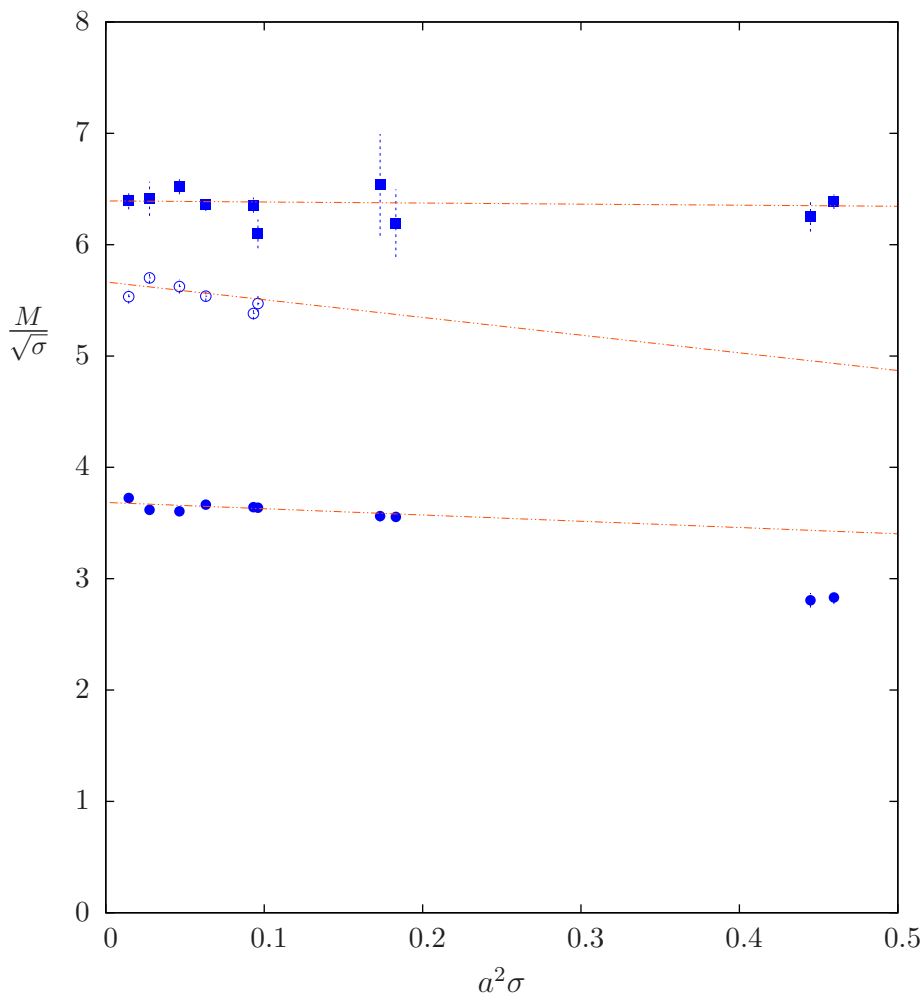


**Figure 3.** Masses of the ground state 0+ ( $\bullet$ ), first excited 0+ ( $\circ$ ), and ground state 2+ ( $\blacksquare$ ) in units of the string tension, plotted versus the string tension, and with  $O(a^2)$  continuum extrapolations shown. All for  $SO(6)$  in  $D=2+1$ .

as displayed in figure 4. Note that we have used the mean-field improved coupling,  $\beta_I = \beta\bar{u}_p = \lim_{a \rightarrow 0} 2N/ag^2$ , which is commonly used to improve the approach to the continuum limit [11, 12]. Taking the  $SU(4)$  value from [11, 12] we find

$$\begin{aligned} \sqrt{\sigma}/g^2 &= 0.4365(19) & SO(6) \\ \sqrt{\sigma_{2A}}/g^2 &= 0.8832(41) & SU(4) \end{aligned} \tag{3.6}$$

which implies that

$$g^2|_{so6} = 2.023(13) g^2|_{su4} \tag{3.7}$$

which is again consistent with eq. (2.12) within 2 standard deviations.

These calculations not only serve to demonstrate the equivalence of  $SO(6)$  and  $SU(4)$  gauge theories at the nonperturbative level where the differing global nature of these groups

$\mu/\sqrt{\tilde{\sigma}}$ , D=2+1			
$\mu$	SO(6)		SU(4)
	$O(a^2)$	$O(a^4)$	
$M_{0+}$	3.675(27)	3.723(47)	3.638(25)
$M_{0+\star}$	5.66(7)	5.52(10)	5.48(5)
$M_{2+}$	6.47(8)	6.39(14)	6.16(8)
$T_c$	0.810(18)		0.817(5)

**Table 3.** Continuum limit of some glueball masses and the deconfining temperature in D=2+1 SO(6) and SU(4) gauge theories, all in units of the string tension  $\tilde{\sigma}$ . In some cases we show  $O(a^4)$  as well as  $O(a^2)$  extrapolations. In SU(4)  $\tilde{\sigma}$  is the k=2 antisymmetric string tension.

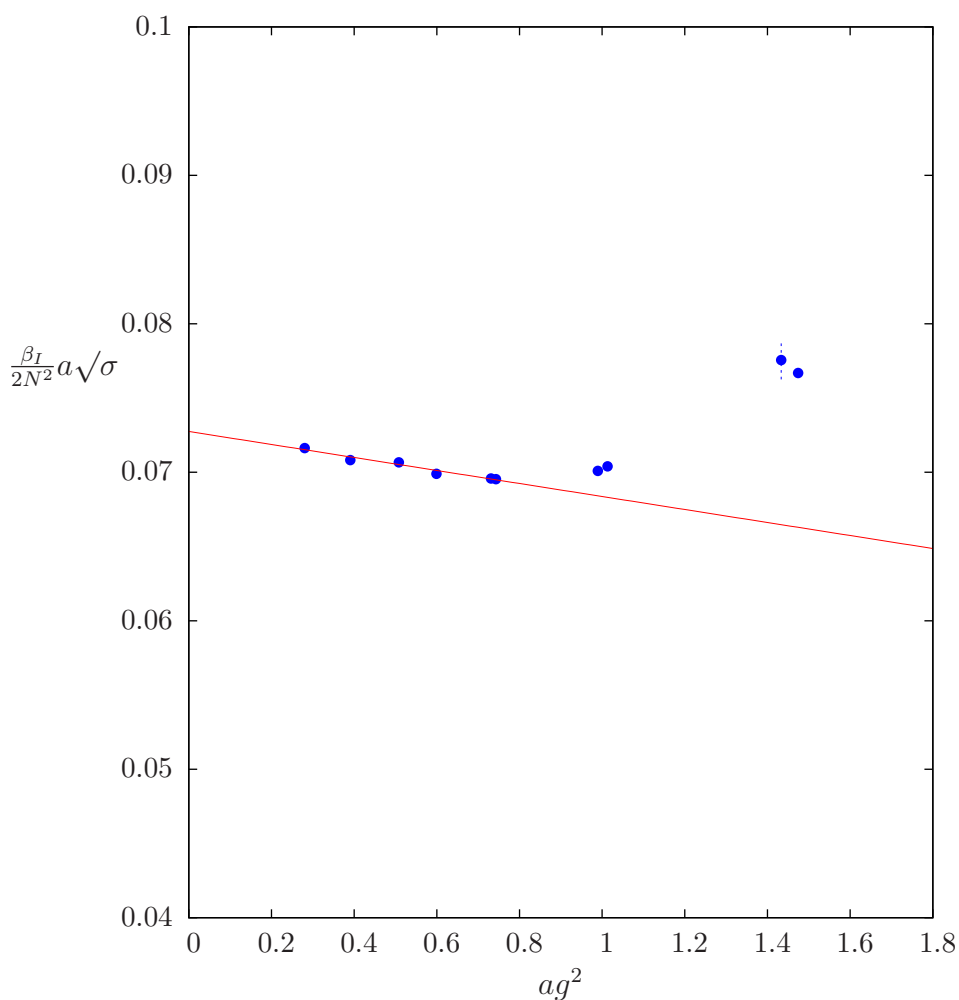


**Figure 4.** String tension in units of  $g^2 N$  (using  $\beta_I = 2N/ag^2$ ) with an  $O(ag^2)$  extrapolation to the continuum limit. For SO(6) in D=2+1.

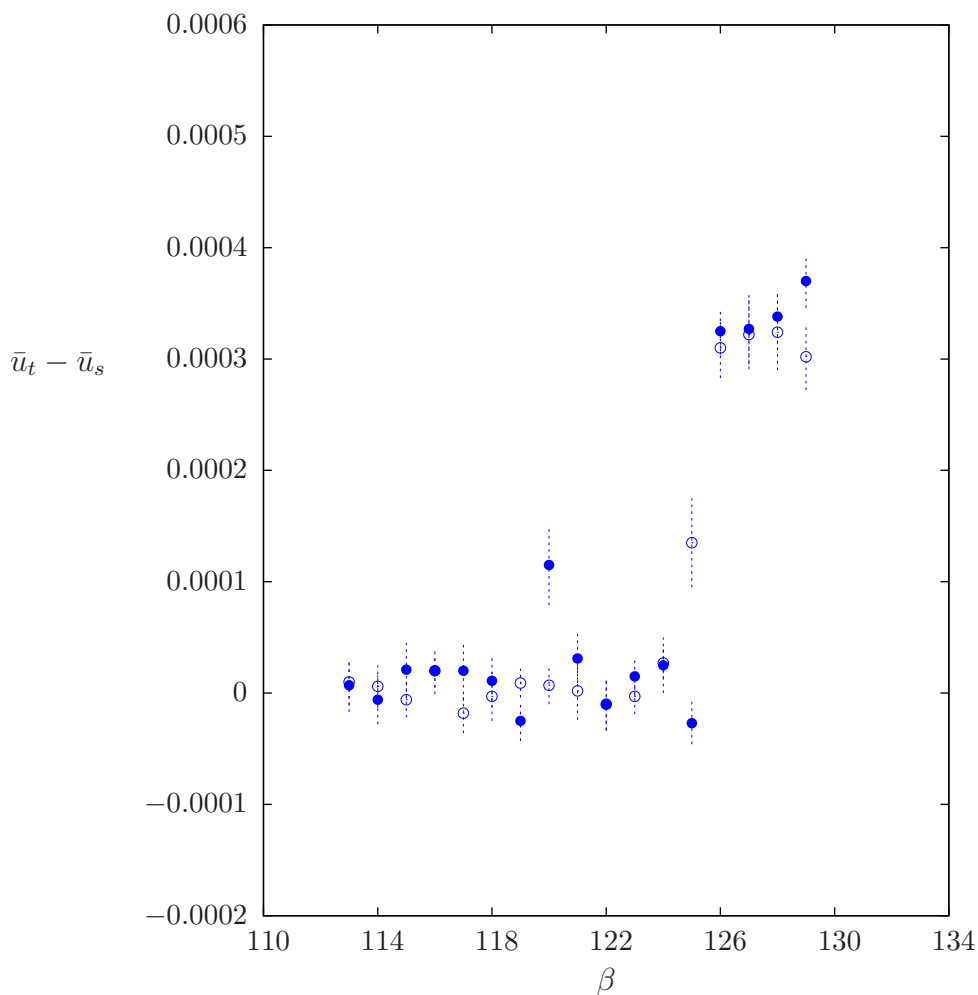


**Figure 5.** Difference between average spatial and temporal plaquettes on a  $20^{25}$  lattice in  $SO(12)$  as  $\beta$  is reduced,  $\bullet$ , and then increased,  $\circ$ .

might have played some role, but they also give us confidence that lattice calculations in  $SO(N)$  gauge theories encounter no hidden obstacles.

### 3.4 The deconfining transition

$SO(2N)$  gauge theories should deconfine at some temperature  $T = T_c = O(\sqrt{\sigma})$  just like  $SU(N)$  gauge theories and we expect deconfinement to coincide with the spontaneous breaking of the  $Z_2$  symmetry. That is to say, one can locate the deconfining transition just as one does for  $SU(N)$ , see e.g. [15–19].

To illustrate the transition we consider a  $20^{25}$  lattice in  $SU(12)$ . In the relevant range of couplings this spatial volume turns out to be large and so we can consider it to be at a well defined temperature  $T = 1/5a(\beta)$ . By varying  $\beta$  we vary  $a(\beta)$  and hence  $T$ . In figure 5 we show the value of the difference between the average spatial and temporal plaquette as we first decrease  $\beta$  and then increase it. At large  $N$ , volume independence tells us that this

$l_t$	SO(4)		SO(6)		SO(8)		SO(12)	
	$\beta_c$	$a\sqrt{\sigma}$	$\beta_c$	$a\sqrt{\sigma}$	$\beta_c$	$a\sqrt{\sigma}$	$\beta_c$	$a\sqrt{\sigma}$
2	6.475(99)	0.628(32)	15.15(15)	0.660(18)	27.35(50)	0.681(25)	63.75(75)	0.651(24)
3	7.45(10)	0.424(11)	17.75(25)	0.427(12)	33.25(75)	0.423(17)	81.25(75)	0.406(9)
4	8.30(20)	0.319(12)	21.75(75)	0.308(7)	41.50(25)	0.307(3)	102.00(75)	0.291(4)
5	9.30(40)	0.265(22)	25.20(60)	0.254(7)	49.75(75)	0.247(4)	125.0(10)	0.2337(20)

**Table 4.** Values of  $\beta$  at which D=2+1 SO( $N$ ) theories reach a temperature  $T_c = 1/a(\beta_c)l_t$  at which they deconfine. The corresponding value of the string tension,  $a^2\sigma$ , is listed.

quantity should be zero in the confining phase, and so in that limit it acts as an exact order parameter. In figure 5 we see a clear transition at  $\beta \sim 125$ . To locate the transition on a spatial volume  $V$  one can form a ‘susceptibility’ from this plaquette difference, calculate its value at several neighbouring values of  $\beta$ , interpolate using reweighting, and define the transition  $\beta_c(V)$  to be the maximum of this susceptibility. One can now repeat this for various  $V$  and extrapolate  $\beta_c(V)$  to  $\beta_c(\infty)$ . This standard strategy, see e.g. [15, 16], can provide very precise values of the critical coupling. However just locating the transition region from scans such as that plotted in figure 5 provides a value of  $\beta_c$  that is accurate enough for our purposes in this exploratory study. In principle one can also attempt to identify the order of the transition by looking for hysteresis effects, but we do not attempt to do so here.

We have performed such scans for  $L_s^2 L_t$  lattices with  $L_t = 2, 3, 4, 5$  and typically for 2 or 3 values of  $L_s$  in each case to check that finite  $V$  corrections are negligible at our level of accuracy. We have simultaneously calculated the string tension at the resulting values of  $\beta_c$  to give us an estimate of  $T_c/\sqrt{\sigma} = 1/\{a(\beta_c)\sqrt{\sigma}L_t\}$ . (The calculations of  $a^2\sigma$  have been performed on lattices with  $L_s\sqrt{\sigma} \in [2.5, 4.0]$  and  $L_t > L_s$ , so that they are effectively at  $T = 0$ .) These values are listed in table 4. We can then extrapolate to the continuum limit using a leading  $O(a^2)$  correction

$$\left. \frac{T_c}{\sqrt{\sigma}} \right|_a \simeq \left. \frac{T_c}{\sqrt{\sigma}} \right|_{a=0} + ca^2\sigma \tag{3.8}$$

We have done this for the SO(4), SO(6), SO(8) and SO(12) gauge theories, and the results, with continuum extrapolations, are shown in figure 6. The resulting continuum values are listed in table 5. Here we also show the known value for SU(4) [17–19] (using the  $k = 2A$  string tension) and we observe that the SO(6) and SU(4) values of  $T_c/\sqrt{\sigma}$  are entirely consistent.

Finally we extrapolate our results to  $N = \infty$  using a leading  $O(1/N)$  correction, as shown in figure 7. This gives us the  $N = \infty$  value displayed in table 5. We list there the SU( $\infty$ ) value [17–19] which we can see is consistent with the SO( $\infty$ ) value, hence providing another confirmation of the large- $N$  equivalence of SU( $N$ ) and SO( $N$ ) gauge theories.

### 3.5 Continuum mass ratios

Our above calculations of  $T_c/\sqrt{\sigma}$  required us to calculate string tensions at values of  $\beta$  close to  $\beta_c$ , where  $a(\beta_c) = 1/L_t T_c$ , with  $L_t \in [2, 5]$ . We calculated glueball masses at the same



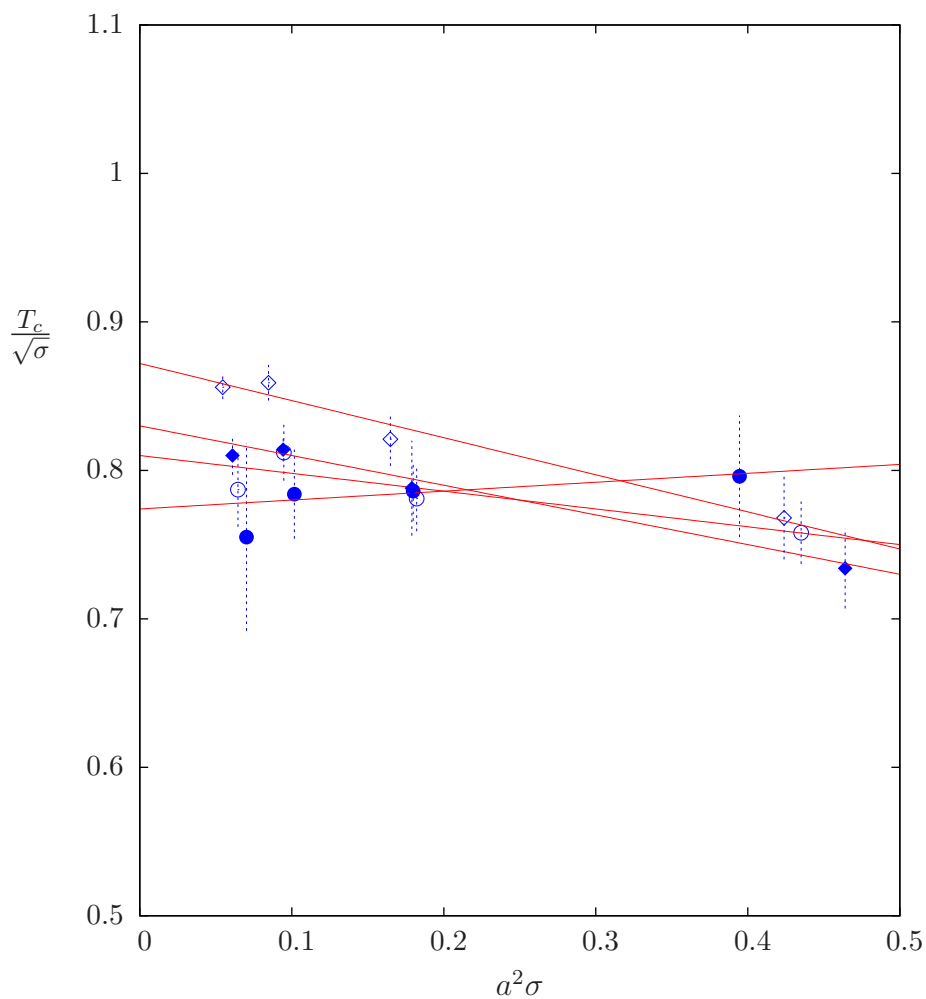


**Figure 6.** Lattice values of the deconfining temperature  $T_c$  in units of the string tension with continuum extrapolations shown. For  $\text{SO}(4)$ ,  $\bullet$ ,  $\text{SO}(6)$ ,  $\circ$ ,  $\text{SO}(8)$ ,  $\blacklozenge$ , and  $\text{SO}(12)$ ,  $\diamond$ .

$\text{SO}(N)$		$\text{SU}(N)$	
$N$	$T_c/\sqrt{\sigma}$	$N$	$T_c/\sqrt{\sigma}$
4	0.774(33)	4	0.817(3)
6	0.810(18)		
8	0.830(11)		
12	0.8715(88)		
$\infty$	0.924(20)	$\infty$	0.903(23)

**Table 5.** Continuum limit of deconfining temperature in units of the string tension for various  $\text{SO}(N)$  gauge theories and the  $N \rightarrow \infty$  extrapolation. For comparison we show the  $\text{SU}(4)$  and  $\text{SU}(\infty)$  values from [17–19].

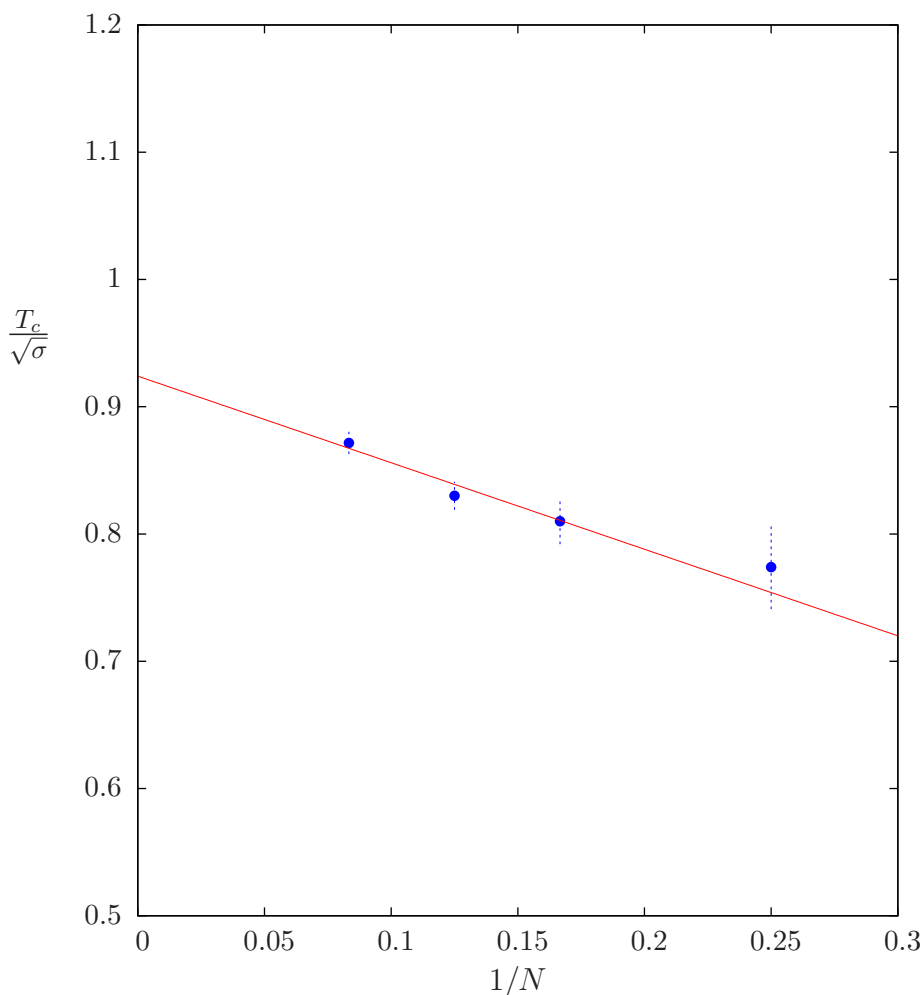


**Figure 7.** Continuum values of the D=2+1 SO( $N$ ) deconfining temperature  $T_c$  in units of the string tension plotted against  $1/N$  with a large- $N$  extrapolation shown.

time, and we will now use these calculations to estimate the continuum limit of various dimensionless physical ratios just as we did earlier for SO(6). Of course the difference with the latter calculation is that the range of  $a$  used for the continuum limit is much smaller now. In fact the bulk ‘transition’,  $\beta_b$ , more-or-less coincides with the deconfining transition,  $\beta_c(L_t)$ , on a lattice with  $L_t = 3$ . Thus, we are not surprised to find that we cannot perform statistically credible continuum extrapolations with weak-coupling corrections if we include the masses at  $\beta \simeq \beta_c(L_t = 2)$ . However we find that extrapolations are often possible from a value of  $\beta \simeq \beta_c(L_t = 3)$ , i.e. from the bulk transition region onwards into weak coupling. Some evidence that we are not being too optimistic is given by our results for SO(6) where we have performed calculations to much weaker couplings. In figure 3, we see that the extrapolations to the continuum of typical mass ratios pass through the  $\beta_c(L_t = 3)$  values but not through the values at  $\beta_c(L_t = 2)$ . For  $\sqrt{\sigma/g^2}$  we see in figure 4

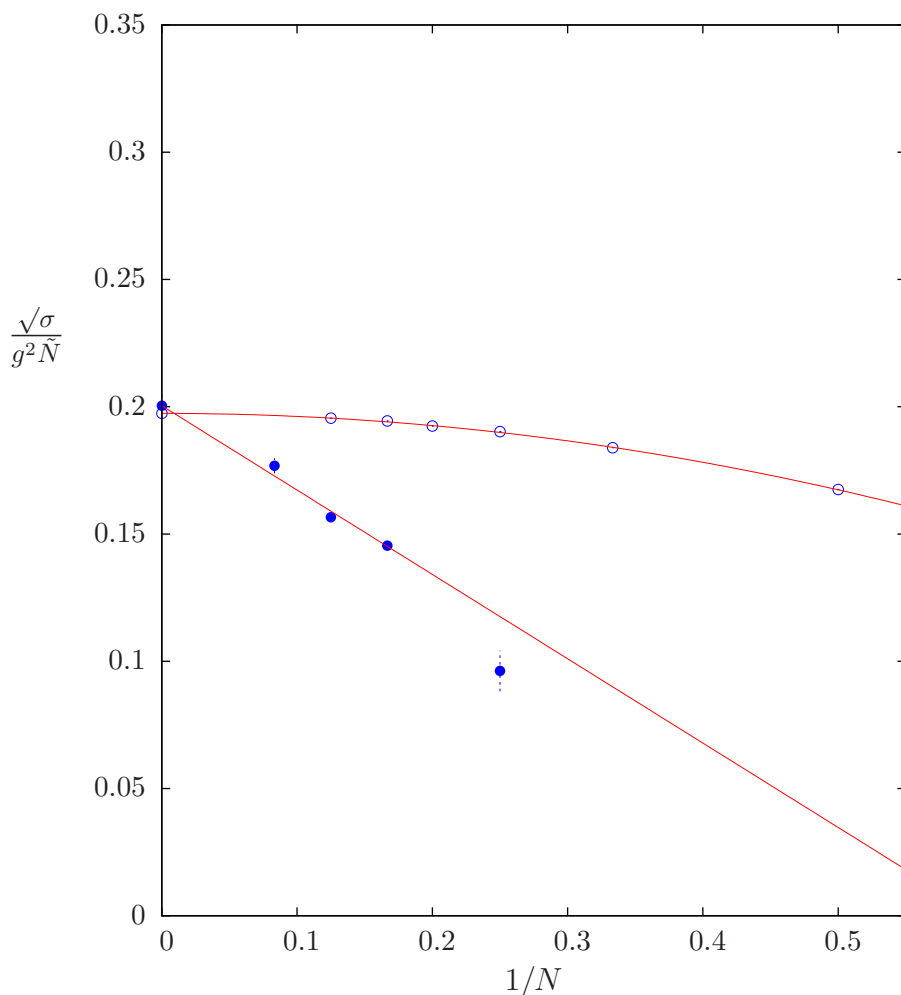


**Figure 8.** The  $SO(N)$  continuum string tension,  $\bullet$ , in units of the 't Hooft coupling modified by using  $\tilde{N} = N/2$ , with an  $O(1/N)$  extrapolation to  $N = \infty$  shown. Also shown are known  $SU(N)$  values,  $\circ$ , in units of the standard 't Hooft coupling,  $\tilde{N} = N$ , and with an  $O(1/N^2)$  extrapolation of these to  $N = \infty$ .

some deviation even from the  $\beta_c(L_t = 3)$  values, but it is not large. So while some of our extrapolations do have a mediocre  $\chi^2$ , most are good, and we can expect the overall picture to be qualitatively reliable.

In figure 8 we display our  $SO(N)$  continuum values for the string tension in units of the 't Hooft coupling,  $g^2 N$ , modified so that  $N \rightarrow N/2$ , i.e. we double the calculated values of  $\sqrt{\sigma}/g^2 N$ . We observe that the values for  $N \geq 6$  [23, 24] can be extrapolated to  $N = \infty$  with just the leading  $O(1/N)$  correction. For comparison we have shown the  $SU(N)$  values, with an unmodified 't Hooft coupling and we show an  $O(1/N^2)$  fit to these. We observe that the  $N = \infty$  extrapolations for  $SO(N)$  and  $SU(N)$  are consistent with each other. The various (unmodified) continuum string tensions for  $SO(N)$  are listed in table 6 as are the continuum extrapolations. Taking into account our other results, this tests the large  $N$

SO(N) , D=2+1				
$N$	$\sqrt{\sigma}/g^2N$	$M_{0+}/\sqrt{\sigma}$	$M_{2+}/\sqrt{\sigma}$	$M_{0+^*}/\sqrt{\sigma}$
4	0.0481(40)	3.366(33)	5.89(8)	—
6	0.0727(4)	3.665(21)	6.36(6)	5.537(43)
8	0.0783(8)	3.547(111)	6.45(15)	5.761(125)
12	0.0884(15)	3.873(82)	6.69(11)	6.025(78)
SO( $\infty$ )	0.1002(23)	4.18(8)	7.13(14)	6.51(16)
SU( $\infty$ )	0.0988(2) $\times 2$	4.11(2)	6.88(6)	6.21(5)

**Table 6.** Continuum limits of various mass ratios for various SO( $N$ ) gauge theories and the  $N \rightarrow \infty$  extrapolations. For comparison we show the known SU( $\infty$ ) values [11, 12, 23, 24].

prediction in eq. (2.1) for the relationship between the SO( $N$ ) and SU( $N$ ) couplings to an accuracy of  $\sim \pm 2\%$ .

In figure 9 we display our SO( $N$ ) continuum values for some of the lightest glueball masses, in units of the string tension. We also show the large  $N$  extrapolations. All these values are listed in table 6 where we also list the corresponding large  $N$  limits for SU( $N$ ) gauge theories [11, 12]. We see a satisfactory agreement at the 2 standard deviation level.

These results confirm, albeit with a modest accuracy, our expectations for the relationship between SU( $N$ ) and SO( $N$ ) gauge theories in 2+1 dimensions.

#### 4 D=3+1

Finally we turn briefly to SO( $N$ ) gauge theories in 3+1 dimensions.

We begin with the strong-to-weak coupling bulk transition which is easy to identify in  $D = 3 + 1$  as it is a strong first-order transition in which the average plaquette undergoes a large and sharp discontinuity even on very small lattices. We have performed calculations where we gradually decrease  $\beta$  through the transition and then, well after that transition, we gradually increase  $\beta$ . Because the transition is strongly first order we have a substantial hysteresis effect, and the two locations of the transitions obtained in this way do not coincide. We list in table 7 the bulk transitions obtained for various SO( $N$ ) groups. These calculations have been mostly obtained on small  $4^4$  lattices, but several checks on larger volumes show that any finite volume corrections are small.

Any continuum extrapolation can only use values of  $\beta$  on the weak-coupling side of the bulk transition. To calculate the continuum physics of the confining phase, the lattice size  $L_s$  must be large enough i.e.  $aL_s > 1/T_c$  at the very least. If the lattice spacing on the weak-coupling side of  $\beta_b$  is very small this may require prohibitively large values of  $L_s$ . Indeed it has long been known that this is the case in SO(3). One can of course improve one's chances by using the strong hysteresis to perform weak-coupling calculations at the largest possible value of  $\beta$ , i.e.  $\beta \simeq \beta_b^\downarrow + \epsilon$ .

This is the value of  $\beta$  at which we have performed some test weak-coupling runs. As expected our test run in SO(3) at  $\beta = 2.52$  on a ‘large’  $32^4$  lattice reveals that we are

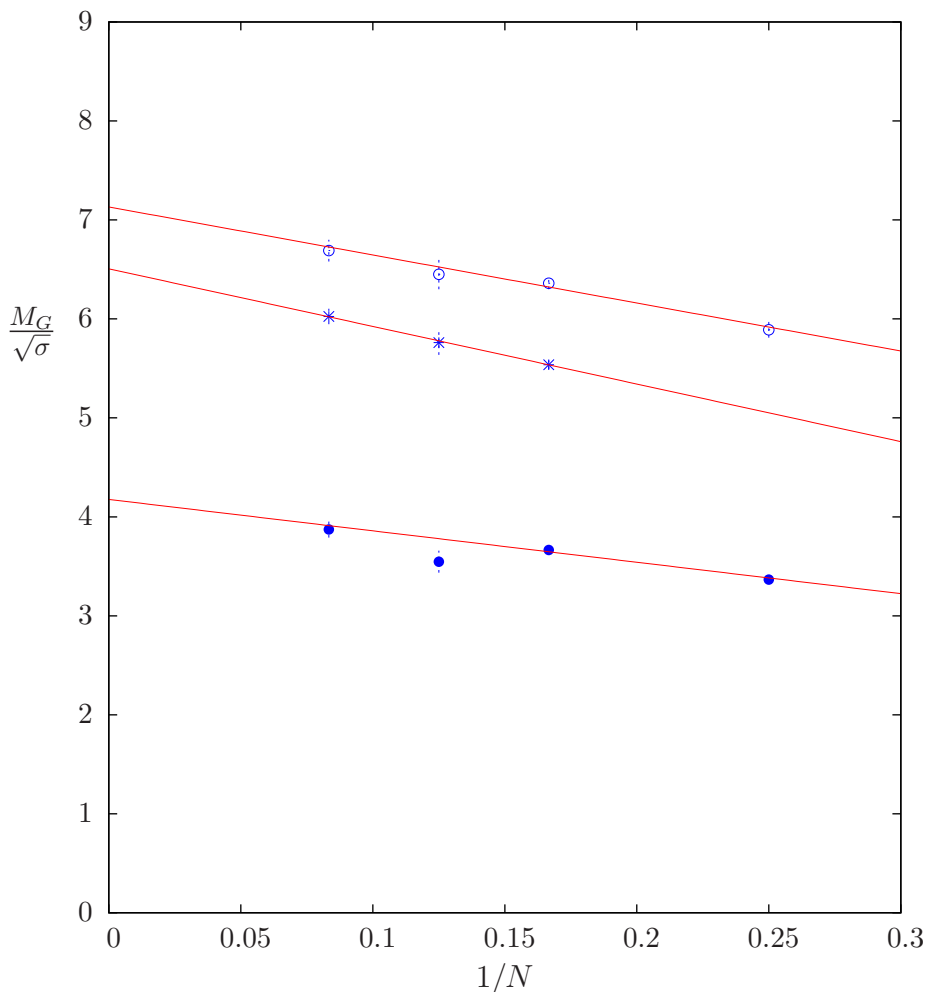


**Figure 9.** Some  $SO(N)$  continuum glueball masses in units of the string tension: the lightest  $0^+$ ,  $\bullet$ , and  $2^+$ ,  $\circ$  and the first excited  $0^+$ ,  $*$ . Large  $N$  extrapolations shown.

in a small-volume phase. The same is true in  $SO(4)$  on a  $32^4$  lattice at  $\beta = 4.75$  where, in addition, we observe the spontaneous breaking of the  $Z_2$  center symmetry. In  $SO(6)$  neither of the  $32^4$  or  $24^3 32$  lattices appear to be clearly large volume. However in  $SO(8)$  we appear to have what looks like the desired confining phase on a  $24^3 32$  lattice at  $\beta = 20$ , although not on a  $16^3 24$  lattice. Here we appear to have  $a\sqrt{\sigma} \simeq 0.16$ . Finally in  $SO(16)$  we find that we can obtain ‘large-volume’ physics on a  $12^3 16$  lattice at  $\beta = 83.5$ , where we find  $a\sqrt{\sigma} \simeq 0.31$ . Here we are beginning to approach the corresponding values found in  $SU(N)$  gauge theories at larger  $N$ . Thus at our larger values of  $N$  one could imagine reducing  $a$  by a further factor of  $\sim 2$  or  $3$  so as to have a useful range of  $a$  for a continuum extrapolation. However one would be reluctant to calculate dynamical fermionic properties at such large  $N$ . We are therefore focusing on improving the action rather than pursuing further calculations with the standard plaquette action.

SO( $N$ ) , D=3+1		
G	$\beta_b \downarrow$	$\beta_b \uparrow$
SO(3)	2.48(1)	2.53(1)
SO(4)	4.62(3)	4.87(3)
SO(5)	7.35(5)	7.95(5)
SO(6)	10.85(5)	11.8(1)
SO(7)	14.77(8)	16.58(8)
SO(8)	19.7(1)	21.9(1)
SO(9)	25.12(12)	28.12(12)
SO(10)	31.12(12)	35.12(12)
SO(16)	82.25(25)	93.25(25)

**Table 7.** Values of  $\beta$  at the bulk transition in various D=3+1 SO( $N$ ) gauge theories obtained mainly on  $4^4$  lattices. Separately for  $\beta$  decreasing and increasing.

D=3+1		
	SO(6)	SU(3)
$M_{2+}/M_{0+}$	1.45(5)	1.35(4)
$T_c/M_{0+}$	2.13(5)	2.29(5)
$M_{0+}/\sqrt{\sigma}$	2.87(6)	3.55(7)

**Table 8.** Comparing some continuum energy ratios in D=3+1 between SU(3) and that expected for SO(6) from its equivalence with SU(4) [10]. (Using the  $k = 2A$  string tension.)

Although we are not yet in a position to compare values calculated within SO(6) with known results for SU(3), we can do so indirectly by predicting the SO(6) physics from the known SU(4) physics [11, 12]. Doing so we have the comparison in table 8. We observe that the physics is very similar except where it involves the string tension, and this is simply because the SO(6) string tension corresponds to the  $k = 2A$  SU(4) string tension.

Finally we comment that, just as for  $D = 2 + 1$ , we can make use of the SO(6)-SU(4) equivalence to predict the physics in  $D = 3 + 1$  of all  $SO(N \geq 6)$  theories if we assume that the leading  $O(1/N)$  correction dominates and input that SO( $N$ ) and SU( $N$ ) gauge theories have a common large- $N$  limit.

## 5 Conclusions

Our aim in this paper has been to review some relevant properties of SO( $N$ ) gauge theories, complemented with some exploratory lattice calculations. This is intended to serve as a useful background for more detailed and precise numerical calculations. Such studies, comparing SO( $N$ ) and SU( $N$ ) pure gauge theories, will provide a starting point for attempts to evade the finite chemical potential sign problem in QCD using the (orbifold) large- $N$  equivalence of SO( $2N$ ) and SU( $N$ ) theories [1, 7].

We have seen, in  $D = 2 + 1$ , that the equivalence of  $\text{SO}(6)$  and  $\text{SU}(4)$  Lie algebras does indeed appear to translate into an equivalence of the spectra — with the string tension of the former corresponding to the lightest  $k = 2$  (antisymmetric) tension in the latter. Since ‘glueball’ mass ratios are very similar in  $\text{SU}(3)$  and  $\text{SU}(4)$  gauge theories this implies that dimensionless mass ratios will also be similar in  $\text{SU}(3)$  and  $\text{SO}(6)$  gauge theories, except where they involve the string tension or the coupling  $g^2$ , where, however, the differences can be predicted.

If, furthermore, one assumes that the leading  $O(1/N)$  correction dominates down to  $N = 6$ , then one can use the  $\text{SO}(6)/\text{SU}(4)$  equivalence and the known  $\text{SU}(4)$  spectrum to predict the spectrum of  $\text{SO}(N)$  gauge theories for all  $N \geq 6$ . (One can additionally use the  $\text{SO}(3)/\text{SU}(2)$  equivalence to pin down both the  $1/N$  and  $1/N^2$  corrections with appropriate assumptions.) Our exploratory  $D = 2 + 1$  calculations of the deconfining temperature,  $T_c$ , the lightest two  $J^P = 0^+$  glueball masses and the lightest  $J^P = 2^+$  glueball mass, indicate that the  $O(1/N)$  correction does indeed dominate all the way down to  $N = 6$  and often down to  $N = 4$ .

This  $\text{SO}(6)/\text{SU}(4)$  spectral equivalence should also hold in  $D = 3 + 1$  and suggests a similarly strong similarity between  $\text{SO}(6)$  and  $\text{SU}(3)$  and similar predictions for  $N \geq 6$  assuming the dominance of the  $O(1/N)$  correction down to  $N = 6$ . Here however our lattice calculations have been obstructed by the first-order strong-weak coupling ‘bulk’ transition. For low  $N$  this is so located that to calculate physics on the weak coupling side would require extremely large lattices. Although we find that for larger  $N$ , e.g.  $\text{SO}(16)$ , this is no longer the case, and the location of the transition in physical units is not much different from that in  $\text{SU}(8)$ , what we would really like to do is to access the continuum physics of lower  $N$   $\text{SO}(N)$  gauge theories, and to that end we are investigating improved actions where the ‘improvement’ desired is to push the bulk transition to stronger coupling.

## Acknowledgments

Our interest in this project was originally motivated by Aleksey Cherman, and we are very grateful for his encouragement and useful advice. The project originated in a number of discussions between two of the authors (FB and MT) and Aleksey Cherman during the 2011 Workshop on ‘Large-N Gauge Theories’ at the Galileo Galilei Institute in Florence, and we are grateful to the Institute for providing such an ideal environment within which to begin collaborations. The numerical computations were mostly carried out on EPSRC and Oxford funded computers in Oxford Theoretical Physics.

## References

- [1] A. Cherman, M. Hanada and D. Robles-Llana, *Orbifold equivalence and the sign problem at finite baryon density*, *Phys. Rev. Lett.* **106** (2011) 091603 [[arXiv:1009.1623](#)] [[INSPIRE](#)].
- [2] S. Kachru and E. Silverstein, *4 – D conformal theories and strings on orbifolds*, *Phys. Rev. Lett.* **80** (1998) 4855 [[hep-th/9802183](#)] [[INSPIRE](#)].
- [3] M. Bershadsky and A. Johansen, *Large-N limit of orbifold field theories*, *Nucl. Phys. B* **536** (1998) 141 [[hep-th/9803249](#)] [[INSPIRE](#)].

- [4] M. Schmaltz, *Duality of nonsupersymmetric large- $N$  gauge theories*, *Phys. Rev. D* **59** (1999) 105018 [[hep-th/9805218](#)] [[INSPIRE](#)].
- [5] M. Ünsal and L.G. Yaffe, *(In)validity of large- $N$  orientifold equivalence*, *Phys. Rev. D* **74** (2006) 105019 [[hep-th/0608180](#)] [[INSPIRE](#)].
- [6] C. Lovelace, *Universality at Large- $N$* , *Nucl. Phys. B* **201** (1982) 333 [[INSPIRE](#)].
- [7] M. Blake and A. Cherman, *Large- $N_c$  Equivalence and Baryons*, *Phys. Rev. D* **86** (2012) 065006 [[arXiv:1204.5691](#)] [[INSPIRE](#)].
- [8] B. Lucini and M. Teper, *SU( $N$ ) gauge theories in four-dimensions: Exploring the approach to  $N = \infty$* , *JHEP* **06** (2001) 050 [[hep-lat/0103027](#)] [[INSPIRE](#)].
- [9] H.B. Meyer, *Glueball Regge trajectories*, [hep-lat/0508002](#) [[INSPIRE](#)].
- [10] B. Lucini, M. Teper and U. Wenger, *Glueballs and  $k$ -strings in SU( $N$ ) gauge theories: Calculations with improved operators*, *JHEP* **06** (2004) 012 [[hep-lat/0404008](#)] [[INSPIRE](#)].
- [11] M.J. Teper, *SU( $N$ ) gauge theories in  $(2+1)$ -dimensions*, *Phys. Rev. D* **59** (1999) 014512 [[hep-lat/9804008](#)] [[INSPIRE](#)].
- [12] B. Lucini and M. Teper, *SU( $N$ ) gauge theories in  $(2+1)$ -dimensions: Further results*, *Phys. Rev. D* **66** (2002) 097502 [[hep-lat/0206027](#)] [[INSPIRE](#)].
- [13] P. de Forcrand and O. Jahn, *Comparison of SO(3) and SU(2) lattice gauge theory*, *Nucl. Phys. B* **651** (2003) 125 [[hep-lat/0211004](#)] [[INSPIRE](#)].
- [14] F. Bursa, R. Lau and M. Teper, in progress.
- [15] B. Lucini, M. Teper and U. Wenger, *The High temperature phase transition in SU( $N$ ) gauge theories*, *JHEP* **01** (2004) 061 [[hep-lat/0307017](#)] [[INSPIRE](#)].
- [16] B. Lucini, M. Teper and U. Wenger, *Properties of the deconfining phase transition in SU( $N$ ) gauge theories*, *JHEP* **02** (2005) 033 [[hep-lat/0502003](#)] [[INSPIRE](#)].
- [17] J. Liddle and M. Teper, *The Deconfining phase transition for SU( $N$ ) theories in  $2+1$  dimensions*, *PoS(LAT2005)* 188 [[hep-lat/0509082](#)] [[INSPIRE](#)].
- [18] K. Holland, *Another weak first order deconfinement transition: Three-dimensional SU(5) gauge theory*, *JHEP* **01** (2006) 023 [[hep-lat/0509041](#)] [[INSPIRE](#)].
- [19] K. Holland, M. Pepe and U.-J. Wiese, *Revisiting the deconfinement phase transition in SU(4) Yang-Mills theory in  $2+1$  dimensions*, *JHEP* **02** (2008) 041 [[arXiv:0712.1216](#)] [[INSPIRE](#)].
- [20] G.'t Hooft, *A Planar Diagram Theory for Strong Interactions*, *Nucl. Phys. B* **72** (1974) 461 [[INSPIRE](#)].
- [21] A. Armoni, M. Shifman and M. Ünsal, *Planar Limit of Orientifold Field Theories and Emergent Center Symmetry*, *Phys. Rev. D* **77** (2008) 045012 [[arXiv:0712.0672](#)] [[INSPIRE](#)].
- [22] H. Georgi, *Lie Algebras in Particle Physics*, Benjamin (1982).
- [23] B. Bringoltz and M. Teper, *Closed  $k$ -strings in SU( $N$ ) gauge theories:  $2+1$  dimensions*, *Phys. Lett. B* **663** (2008) 429 [[arXiv:0802.1490](#)] [[INSPIRE](#)].
- [24] B. Bringoltz and M. Teper, *A Precise calculation of the fundamental string tension in SU( $N$ ) gauge theories in  $2+1$  dimensions*, *Phys. Lett. B* **645** (2007) 383 [[hep-th/0611286](#)] [[INSPIRE](#)].



- [25] H.B. Meyer and M.J. Teper, *High spin glueballs from the lattice*, *Nucl. Phys. B* **658** (2003) 113 [[hep-lat/0212026](#)] [[INSPIRE](#)].
- [26] A. Athenodorou, B. Bringoltz and M. Teper, *Closed flux tubes and their string description in  $D = 3 + 1$   $SU(N)$  gauge theories*, *JHEP* **02** (2011) 030 [[arXiv:1007.4720](#)] [[INSPIRE](#)].
- [27] A. Athenodorou, B. Bringoltz and M. Teper, *Closed flux tubes and their string description in  $D = 2 + 1$   $SU(N)$  gauge theories*, *JHEP* **05** (2011) 042 [[arXiv:1103.5854](#)] [[INSPIRE](#)].
- [28] O. Aharony and M. Dodelson, *Effective String Theory and Nonlinear Lorentz Invariance*, *JHEP* **02** (2012) 008 [[arXiv:1111.5758](#)] [[INSPIRE](#)].
- [29] F. Bursa and M. Teper, *Strong to weak coupling transitions of  $SU(N)$  gauge theories in  $2+1$  dimensions*, *Phys. Rev. D* **74** (2006) 125010 [[hep-th/0511081](#)] [[INSPIRE](#)].
- [30] D. Gross and E. Witten, *Possible Third Order Phase Transition in the Large- $N$  Lattice Gauge Theory*, *Phys. Rev. D* **21** (1980) 446 [[INSPIRE](#)].